

# Applications of Artificial Neural Network and Wavelet Transform For Condition Monitoring of the Combined Faults of Unbalance and Bearing Clearance

H. K. Srinivas<sup>1</sup>, Shamanth. S. Holla<sup>2</sup>, Karthik. B. S<sup>3</sup>, Niroop.S<sup>4</sup>, Chiranjeevi. D<sup>5</sup>  
<sup>1</sup> (Head, Department of Mechanical Engineering, YDIT, Bangalore, Karnataka, India)  
<sup>2,3,4,5</sup> (Students, Department of Mechanical Engineering, YDIT, Bangalore, Karnataka, India)

**Abstract:** The vibration analysis of rotating machinery indicates of the condition of potential faults such as unbalance, bent shaft, shaft crack, bearing clearance, rotor rub, misalignment, looseness, oil whirl and whip and other malfunctions. More than one fault can occur in a rotor. This paper describes the application of Artificial Neural Network (ANN) and Wavelet Transform (WT) for the prediction of the effect of the combined faults of unbalance and bearing clearance on the frequency components of vibration signature of the rotating machinery. The experimental data of frequency components and corresponding Root Mean Square (RMS) velocity (amplitude) data are used as inputs to train the ANN, which consists of a three-layered network. The ANN is trained using an improved multilayer feed forward back propagation Levenberg-Marquardt algorithm. In particular, an overall success rates achieved were 99.78% for unbalance, 99.81% bearing clearance, and 99.45% for the combined faults of unbalance and bearing clearance. The wavelet transform approach enables instant to instant observation of different frequency components over the full spectrum. A new technique combining the WT with ANN performs three general tasks data acquisition, feature extraction and fault identification. This method is tested successfully for individual and combined faults of unbalance and bearing clearance at a success rate of 99.99%.

**Keywords:** Artificial Neural Networks, Rotor faults, Rotor test rig, Unbalance and bearing clearance, Vibration analysis and Wavelet.

## I. INTRODUCTION

In order to avoid the failure of various types of rotating machinery, including mechanical and electrical ones, using sophisticated instrumentation to monitor the condition of various machine signatures has been found to be of considerable use. Vibration measurement and analysis has been applied with success [1] to machines such as steam and gas turbines, pumps, Compressors and induction motors. Faults such as unbalance, misalignment, looseness, rub and cracks generate vibration signals. In the present work, an experimental study has been carried out for a steady state response (constant speed of 1500 rpm) of the rotor for different unbalance masses and bearing clearance on the rotor test rig. The vibration frequency components recorded in the horizontal, vertical and axial directions for the analysis are applied. The experimental study has also been carried out to discover the difference in vibration characteristics due to the combined faults of unbalance and bearing clearance. The monitoring of the vibration of rotating machines has been reported as being a useful technique for the analysis of their condition [2] [3] [4] [5]. Vibration condition monitoring as an aid to fault diagnosis is examined by Taylor (1995), Smalley and colleagues (1996) present a method of assessing the severity of vibrations in terms of the probability of damage by analyzing the vibration signals. Though the measured vibration signatures of frequency domain features are adequate to identify the faults, there is a need for reliable, fast and automated procedure of diagnostics [6]. Unbalance is an important cause of vibration in rotating machinery, and the reduction of such vibration by balancing needs attention. In this paper the experimental studies are presented in the dynamic balancing of flexible shaft using the four run method (FRM) (Mallik & Basu). The vibration frequency of rotor unbalance is synchronous, i.e., one time the shaft rotation speed (1X rpm Rotor unbalance has been reported to appear occasionally in the frequency domain as a series of harmonics of the shaft running speed, i.e., 1Xrpm, 2Xrpm, 3Xrpm, 4Xrpm, etc. [7].

**1.1. Artificial Neural Networks**

The neural network techniques are used in conjunction with signal analysis techniques for classification and quantification of faults [8] in some applications. Kaminski [9] has developed neural networks to identify the approximate location of damage due to cracks through the analysis of changes in the neural frequencies. McCormick and Nandi [10] have used neural network method for automatically classifying the machine condition from the vibration time series. Vyas and Satish Kumar [11] have carried out experimental studies to generate data for rotating machinery faults such as mass unbalance, bearing cap loose. Srinivasan [12] carried out extensive studies on faults like parallel misalignment, angular misalignment, unbalance, crack, light and heavy rubs, looseness and bearing clearance.

The Fig-1 shows a simple network consisting of three layers with one input layer, one hidden layer and one output layer. There are no connections between nodes in the same layer and no connection that bridge the layers. Such networks with only one hidden layer can uniformly approximate any continuous function and therefore provide a theoretical basis for the use of this type of network. The input-output relationship of each node is determined by a set of connection weights  $W_i$ , a threshold parameter  $b_i$  and a node activation function  $A(.)$  such that-

$$Y = A (W_i X_i + b_i) \tag{1}$$

Where  $Y$  is the output of the node and  $X_i$  are the inputs. The activation function  $A(.)$  defines the output of a neuron in terms of activity level at its input. The sigmoid function is the most common activation function used in neural networks. It is defined as a strictly increasing function that exhibits smoothness and asymptotic properties. The Tan-sigmoid activation function is used in the hidden layer. The purelin activation function is used in the output layer.

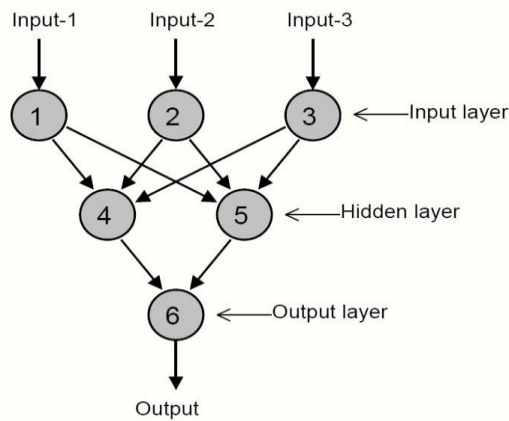


Fig-1 Three- layers network

In the present work, improved back propagation neural network has been applied for the diagnosis of combined faults of unbalance and bearing clearance. It attempts to minimize the square of the error between the output of the network and the desired outputs by changing the connection weights that use some form of gradient descent. The back propagation method has used gradient descent techniques, which are simply the techniques, where parameters such as weights and biases are moved in the opposite direction towards the error gradient. The Levenberg-Marquardt algorithm has the best convergence speeds for small and medium size networks [13, 14]. This optimization technique is more accurate and faster than gradient descent method. The Levenberg-Marquardt update rule is-

$$\Delta W = ( J^T J + \Delta\mu I) J T e \tag{2}$$

Where  $\Delta W$  = Small change in weight.  $J$  is the  $n$  by  $m$  Jacobian matrix  $J^T J$  to keep function  $N$  rows of  $J$  linearly independent and  $\mu$  is a small positive constant chosen to ensure  $(J^T J + \mu I)$  is positive for all 'n' values. If  $\mu$  is very large the above expression approximates gradient descent; if it is small, the above expression becomes the Gauss-Newton method. The Gauss-Newton method is faster, more accurate and near to an error minimum. Training continues until the error goal is met, the minimum error gradient occurs, the maximum value of  $\mu$  occurs, or the maximum number of epochs has been finished. The MAT LAB Neural Network toolbox has been applied for diagnosing the rotating machinery faults.

## 1.2. Wavelet transform

The wavelet transform acts as a “Mathematical microscope” in which one can observe different paths of the signal by “adjusting the focus”. A frequency component of the RMS velocity indicates the health of a particular machine. The wavelet transform approach allows the detection of short-lived frequency component in the signals. The method is logical since high frequency components (such as short bursts) need high frequency resolution as compared with low-frequency components, which require low-frequency resolution. This paper also describes the use of wavelet transform to decompose the vibration signal into several frequency ranges at different level of resolution. The strength (RMS) of the selected decomposed signals is then calculated under combined faults of unbalance mass and bearing clearance conditions. The neural network is then trained with the generated database to automate the fault diagnostic process.

## II. Description Of The Test Rig

The experimental operator is shown in Fig.2. The experimental rotor system used in this work consisted of a motor, which was connected by a flexible coupling and a single disk rotor. The rotor shaft was supported by two identical brass bush bearings and had a length of 250 mm. The diameter of the rotor shaft was 15 mm. It has a disk of 116 mm in diameter, 22 mm in thickness and a disk of mass 1.65 kg which were mounted on the rotor shaft mid-way between the bearing supports. The disk was fixed on the rotor shaft by radial screws. There were 36 tapped holes symmetrically placed on each side of the disk flat faces at a radius of 45 mm in order to attach any desired amount of unbalance mass. The bearing pedestals are provided in order to fix the sensors and measure the dynamic vibration level in the horizontal, vertical and axial directions. The rotor shaft was driven by a 0.37 kW ac/dc variable speed motor. A constant operating speed of 1500 rpm was maintained, though motor speeds ranged from 0-8000 rpm. The natural frequency of the rotor was 4.45Hz in the lateral mode. The critical speed was 267 rpm.

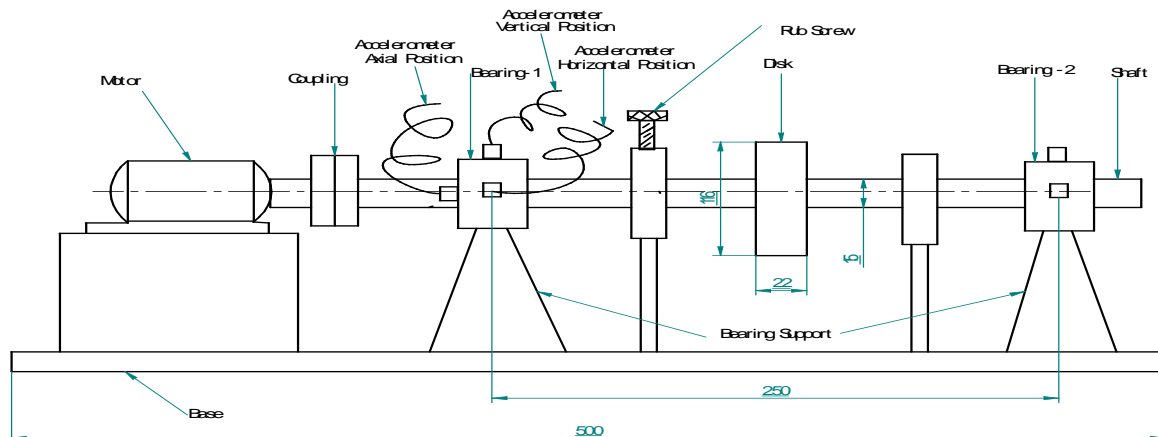


Fig - 2. Rotor Test-Rig

The piezoelectric accelerometers (Bruel & Kjaer, type 4370 piezoelectric accelerometer, Charge Sensitivity 9.99 Picocolumbs/ms<sup>2</sup>) were attached in three directions for measurement of RMS velocity in mm/s. The frequency analysis was carried out using a FFT analyzer (pulse lite, Basic 2-Channel, Max 12K points up to 1000 Hz in put frequency). An accelerometer enables measurement of the vibration level in the horizontal, vertical and axial directions. The output of the accelerometer was connected to the FFT analyzer for frequency analysis. Three special fixtures attached tightly to the bearing pedestal were used to hold the accelerometer at the desired locations. The signal was transmitted to a transducer and pre-amplifier. The output of the pre-amplifier signal was transmitted to the FFT analyzer.

## III. Frequency Spectrum Analysis On Effects Of Combined Faults of Unbalance and Bearing Clearance

In this experiment, combination of mass unbalance and bearing clearance are both introduced simultaneously in the rotor test rig. The unbalance mass ranging from 6.5 g to 18.5g and bearing clearance ranging from 0.02 to 0.08 mm, with a combination of unbalance and bearing clearance were used. In order to investigate the vibration characteristics due to combined unbalance and bearing clearance faults were simulated in the rotor test rig. Initially, the brass bush of bearing clearance of 0.02 mm is used in the rotor test

rig. The unbalance of 6.5 g, 10.5 g, 14.5 g and 18.5 g were created by fixing the unbalance masses at a radius of 45 mm on the periphery of the rotor. The rotor is run at 1500 rpm. The vibration signatures were recorded in horizontal, vertical and axial direction. The frequency analysis has been carried out. The experiments also have been carried out for the bearing clearance of 0.04 mm, 0.06 mm and 0.08 mm by varying the unbalance masses. The frequency components are shown in the Table 1. The graphs of frequency components of RMS velocities are shown in Figure 3(a) to 3(d).

The unbalance mass range was from 6.5 g to 18.5 g with a combination of unbalance and bearing clearance. The machine was run at 1500 rpm. It is observed that the first harmonic in the horizontal direction 1X component has increased from 0.421mm/s to 0.874mm/s. The second harmonic 2X has also increased from 0.029mm/s to 0.147mm/s. There is an increase in the level of 1X frequency component of vibration from 0.234 to 0.346mm/s in vertical direction. The 2X frequency component of vibration has also shown an increasing trend from 0.029 mm/s to 0.159mm/s in the vertical direction. It has been observed from Fig. 3(a) to 3(d) that 1X frequency component of vibration is to be seen predominant in the horizontal direction ranging from 0.421mm/sec to 0.978mm/sec for the bearing clearance ranging from 0.02 mm to 0.08 mm and unbalance ranging from 6.5g to 18.5g corresponding to a speed of 1500 rpm, phase angle of 48 degrees. The increase in the vibration level is the highest with 1X frequency components in the horizontal direction is 0.978 mm/sec.

Table 1: Values of frequency components of RMS vibration velocity (mm/s) for various unbalance mass ranging from 6.5 to 18.5 g and bearing clearance 0.08 mm were obtained at a rotor speed of 1500 rpm.

Frequency components	Unbalance mass in (g) and bearing clearance in (mm)			
	Training set		Testing set	
	6.5+0.08	10.5+0.08	14.5+0.08	18.5+0.08
1XH	0.544	0.622	0.902	0.978
2XH	0.056	0.052	0.134	0.182
3XH	0.036	0.034	0.124	0.166
4XH	0.028	0.028	0.068	0.078
1X V	0.342	0.382	0.462	0.524
2X V	0.046	0.072	0.158	0.198
3X V	0.034	0.041	0.148	0.154
4X V	0.026	0.036	0.084	0.084
1X A	0.072	0.089	0.096	0.098
2X A	0.058	0.066	0.088	0.082
3X A	0.042	0.058	0.066	0.036
4X A	0.036	0.042	0.054	0.054

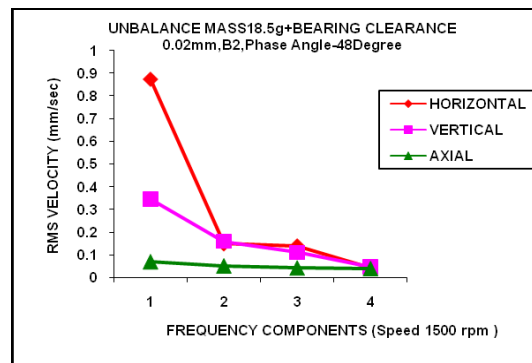
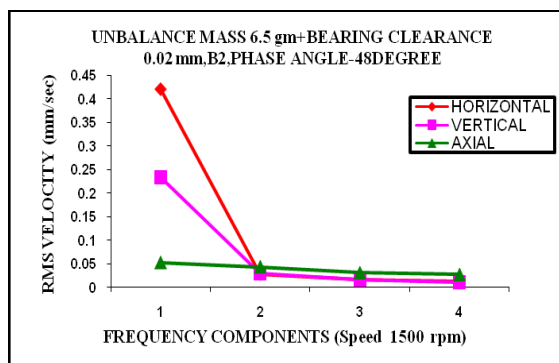


Fig. 3(a). Frequency components of RMS velocity for unbalance mass 6.5g & bearing clearance 0.02mm (L).  
 Fig. 3(b). Frequency components of RMS Velocity for unbalance mass 18.5g & bearing clearance 0.02mm (R).

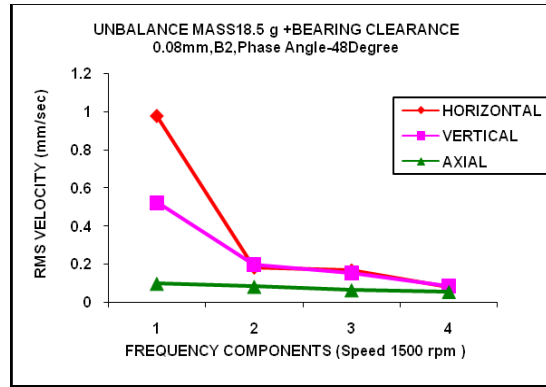
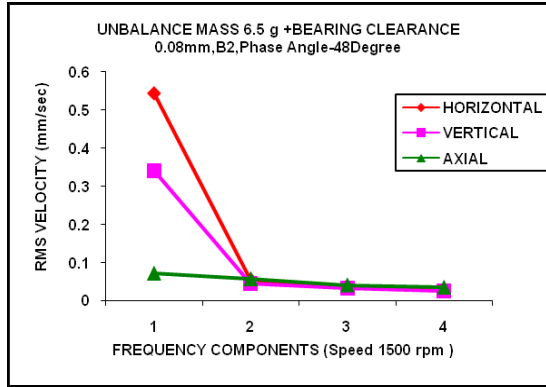


Fig. 3(c). Frequency components of RMS Velocity for unbalance mass 6.5g & bearing clearance 0.08mm (L).  
 Fig. 3(d). Frequency components of RMS Velocity for unbalance mass 18.5g & bearing clearance 0.08 mm(R).

#### IV. Applications of A.N.N. For Fault Diagnosis

The neural network used for rotor fault diagnosis consisted of one hidden layer and one output layer. Tan-sigmoid activation function was used in the hidden layer. The output layer used a purelin transfer function. The input vectors for training the network were the RMS velocity (mm/s) frequency components of the vibration signatures measured in the horizontal, vertical and an axial direction for faults such as unbalance and bearing clearance. The network performance is called generalization, which is the ratio of actual output to the desired output expressed in a percentage. The network was trained and tested with different neuron combination with different error goals for the above faults.

##### 4.1. Network training and testing of combined faults of unbalance and bearing clearance data

The training and test data of the present study were generated on a rotor test rig (shown in Fig.2). Table-1 shows the training data and test data of RMS velocity for various unbalance masses and bearing clearance in the horizontal, vertical and axial directions. The values of frequency components in the horizontal, vertical and axial directions for unbalance ranging from 6.5g to 18.5g are noted. The ANN was trained by using MAT LAB Neural Network Tool Box. The ANN is said to be trained when the epochs are maximum, learning rate  $\mu$  is maximum and error is minimum. The training was carried out using of error goals from 0.01 to 0.0001, with different number of neurons. Since there is no specific method to decide the exact number of neurons in the hidden layer, an empirical geometrical pyramid rule will be discussed [3]. Number of hidden neurons =  $\sqrt{mn}$ , Where  $m$  = number of output neurons,  $n$  = number of input neurons. In this case the value of  $m = 3$ , and  $n = 12$ . According to the empirical rule the number of hidden neurons will be 6. The network was trained using 6 neurons with error goal combinations of 0.0001. The testing was carried out using the test set given in the last column of Table 1. From Table 1, with error goal of 0.0001 and 6 neurons, it is seen that in training number 2, the epochs and ( $\mu$ ) remaining constant the sum squared error becomes minimized, which leads to a good generalization. After successful training, the network is tested for simulation with a separate set of untrained data. It is observed that the neural network is able to detect the corresponding unbalance of 18.4909g and bearing clearance of 0.0798mm for epochs of 4 and an error of 4.69917e-006 for an error goal of 0.0001. The experimental value of unbalance is 18.5g and the value of bearing clearance is 0.08mm. The ANN has identified the value of unbalance to an accuracy of 99.95% and bearing clearance of 99.75%. This is in close correlation with the experimental values. This data is shown in Table 2.

Table 2: Quantification of unbalance mass and bearing clearance, error goal 0.0001 and hidden neurons 6

Serial no.	Experimental values of unbalance mass (g) + bearing clearance (mm)	Epochs	MSE	ANN Quantification values	Percentage
1	6.5	4	0.00108642	6.4458	99.16
	0.02			0.0198	99.00
2	18.5	5	5.97176 e-006	18.4259	99.60
	0.02			0.01970	98.50
3	6.5	12	8.84591e-008	6.4953	99.93
	0.08			0.0796	98.50
4	18.5	4	4.69917e-006	18.4909	99.95
	0.08			0.0798	99.75

### V. Wavelet Analysis

Wavelet transform is a mathematical tool with a powerful structure and enormous freedom to decompose a given signal into several scales at different levels of resolution Figure 5 (a) shows the multi-resolution signal decomposition algorithm used for implementation of discrete wavelet transform. In this figure,  $s^d(n)$  is the sampled signal of  $f(t)$ , sampled at the rate of “ $fs$ ” Hz. The digitized signal  $s(n)$  is then first decomposed into  $a1(n)$  and  $d^1(n)$  using low pass filter  $h1(n)$ , and high pass filter  $g1(n)$ , respectively, where,  $d1(n)$  is called the detail function containing higher frequency terms, and  $a1(n)$  is called the approximation signal containing low frequency terms. This is called first- scale decomposition. The second scale decomposition is now based on the signal  $a1(n)$  which gives  $a_2(n)$  and  $d_2(n)$ . The next higher scale decomposition is now based on  $a_j(n)$  and so on. At any level “ $f$ ” the approximation signal  $a_f(n)$  will be composed of frequencies  $0-f_c$  Hz. Similarly the detail signal  $d_j(n)$  at any level “ $f$ ” will contain frequencies of range  $f_c-2$  Hz. The cut-off frequency “ $f_c$ ” of approximation signal  $a_j(n)$  for a given level  $f$  is found by-

$$f_c = fs/2^{f+1} \tag{3}$$

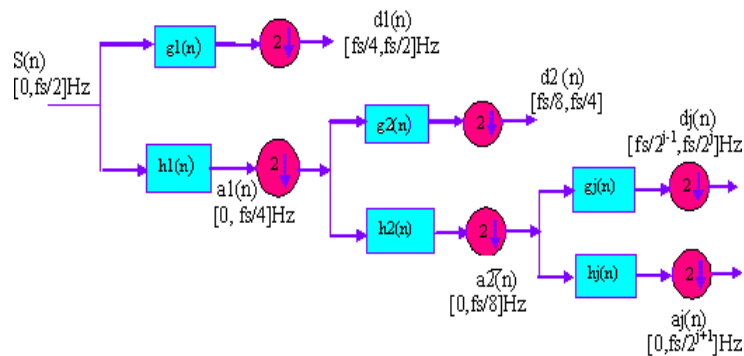


Figure.5 (a). Multi-resolution signal decomposition

Also, the number of points in the decomposed detail and approximation signals decreases gradually through successive decimation. Thus, to compute the Discrete Wavelet Transform (DWT) all that is needed are filters. The signal is convolved with these filters. In contrast to the Short Time Fourier Transforms (STFT), the time resolution becomes arbitrarily fine at high frequency, while the frequency resolution becomes arbitrarily fine at low frequencies. In the present work attempt is made to use wavelet transform for identification of rotor fault, which does not depend on a single frequency, but on a band of frequencies

#### 5.1. Feature Extraction

The aim of the feature extraction is to apply the transformation that extracts the signal features hidden in the original frequently domain. Corresponding to different characteristics of the signal, transformation should be properly selected so that the specific signal structure can be enhanced in its transformed domain. The fault identification techniques are those, which compares current data with that of the known cases to reach the final diagnosis. A multi-resolution property of the discrete wavelet transform (DWT) is used to analyze the vibration signal under different fault conditions. The Daubechies wavelet was selected for the signal analysis because it provides a much more effective wavelet than that obtained with the other wavelets (Haar, Coifman, etc.).When vibration signals collected under different conditions are decomposed via the wavelet, the appreciable differences between the corresponding wavelet coefficients, as shown in Figures. 5(b), (c), (d), and (e), can be seen. However, conducting a direct assessment from all wavelet coefficients turns out to be tedious job. Therefore, the wavelet node power  $e_j$  at “ $f$ ” level decomposition is defined as  $e_j = 1/N_j$

Here,  $N_j$  is the number of coefficients at level “ $f$ ”  $w_{j,k}$  is the  $k^{th}$  coefficient calculated for  $j^{th}$  level,  $e_j$  is the RMS (root mean square) value of the decomposed signal at a level “ $f$ ”. It measures the signal power contained in the specified frequency band indexed by the parameter “ $f$ ”. In order to relate the RMS value of the wavelet decomposition signals with different rotor faults. For each case four sets of data are recorded

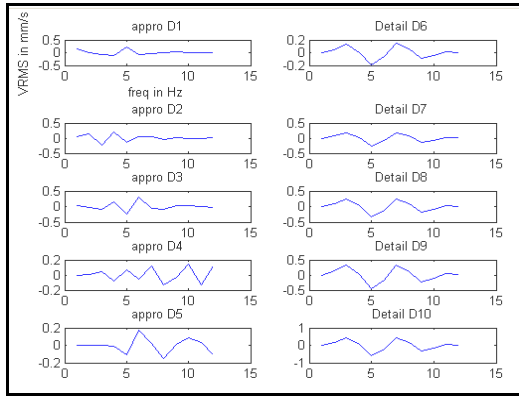


Fig. 5(b) Wavelet decomposition corresponding to unbalance mass 6.5g + bearing clearance 0.08 mm

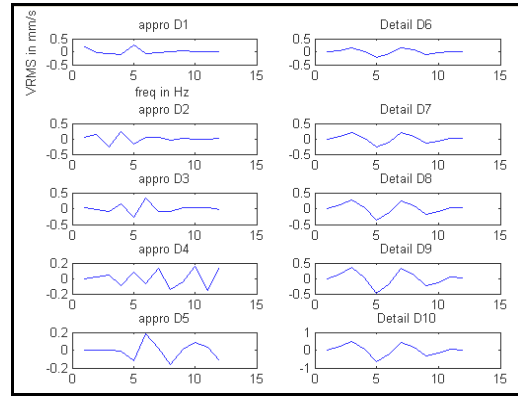


Fig. 5(c) Wavelet decomposition corresponding to unbalance mass 10.5g + bearing clearance 0.08 mm

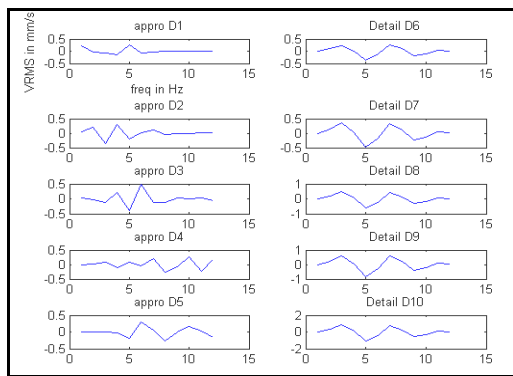


Fig.5 (d) Wavelet decomposition corresponding to unbalance mass 14.5g + bearing clearance 0.08 mm

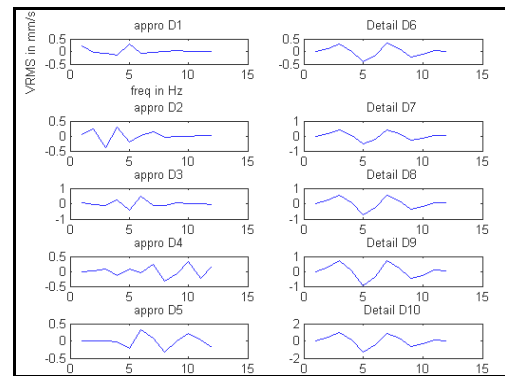


Fig.5 (e) Wavelet decomposition corresponding to unbalance mass 18.5g + bearing clearance 0.08 mm

The vibration in RMS value of first ten decomposition for one segment from each case is shown in Table 3 the similar values are obtained for other vibration segments. From Table 1, it is clearly observed that the bearing clearance is kept constant at 0.08 mm and the unbalance mass is varies from 6.5g to 18.5g in order to study the vibration characteristics due to combination of unbalance and bearing clearance. Due to increase of unbalance mass with constant bearing clearance the 1X frequency component of RMS velocity is predominant in the horizontal direction.

Table 3: RMS value of vibration signal and its ten detailed coefficient wavelet decompositions

Unbalance Mass (g) + Bearing Clearance (mm)	Original RMS	D1	D2	D3	D4	D5
Unbalance Mass 6.5g + Bearing Clearance 0.08 mm	0.1252	0.0278	0.0405	0.0541	0.0301	0.0240
Unbalance Mass 10.5 g + Bearing Clearance 0.08 mm	0.1625	0.0351	0.0549	0.0710	0.0388	0.0284
Unbalance Mass 14.5 g + Bearing Clearance 0.08 mm	0.3635	0.0444	0.0943	0.1393	0.0877	0.0762
Unbalance Mass 18.5 g + Bearing Clearance 0.08 mm	0.4016	0.0523	0.1031	0.1575	0.1141	0.1019

Unbalance Mass (g) + Bearing Clearance (mm)	D6	D7	D8	D9	D10
Unbalance Mass 6.5g + Bearing Clearance 0.08 mm	0.0283	0.0493	0.0899	0.1545	0.2738
Unbalance Mass 10.5 g + Bearing Clearance 0.08 mm	0.0326	0.0569	0.1040	0.1784	0.3163
Unbalance Mass 14.5 g + Bearing Clearance 0.08 mm	0.0970	0.1704	0.3067	0.5302	0.9376
Unbalance Mass 18.5 g + Bearing Clearance 0.08 mm	0.1335	0.2347	0.4207	0.7287	<b>1.2877</b>

**5.2. Data Normalization**

During training of the neural network, input variables of higher values may tend to suppress the influence of the smaller one. To overcome this problem and in order to make neural network perform well, the data must be well processed and properly scaled before input into the ANN. All the components of feature vector are normalized using the following equation-

$$x_n = \left[ \frac{x}{1.5 \times x_{max}} \right] 0.8 + 0.1 \quad (4)$$

Where, x is actual data,  $x_{max}$  is the maximum value of the data and  $x_n$  is the normalized data. The maximum value is obtained from the faulty data set. The maximum value is multiplied by the factor 1.5 so that if the fault severity is more than what is consider until now, the same neural network can be useful for fault identification. Table 4 shows the normalized value of RMS level given in Table 3 by using equation 3. The neural network tool box of MATLAB has been used to simulate the desired network. The “newff” function of MATLAB has been used to create three- layered back propagation network. In the training process, the network is trained according to Levenberg-Marquardt optimization technique until the mean square error is found below 0.0001 or the maximum number of epoch’s (300) is reached.

Table 4: Normalized training data set

Sl. No	Unbalance Mass + Bearing Clearance	Input									
		W1	W2	W3	W4	W5	W6	W7	W8	W9	W10
1	Unbalance Mass 6.5g + Bearing Clearance 0.08 mm	0.1115	0.167	0.1224	0.1124	0.1099	0.1118	0.1204	0.1372	0.1639	0.2134
2	Unbalance Mass 10.5g+Bearing Clearance 0.08mm	0.1145	0.1227	0.1294	0.1160	0.1117	0.1135	0.1235	0.1430	0.1734	0.2310
3	Unbalance Mass 14.5g + Bearing Clearance 0.08mm	0.1183	0.1390	0.1576	0.1363	0.13125	0.1401	0.1705	0.2270	0.3195	0.4883
4	Unbalance Mass 18.5g + Bearing Clearance 0.08mm	0.1216	0.427	0.1652	0.1472	0.1422	0.1552	0.1972	0.2742	0.4018	0.6333



Table 5: Quantification of combined faults of unbalance and bearing clearance using combined form of ANN and Wavelet transform, error goal of 0.0001 and hidden neurons 6

Serial no.	Experimental values of combined faults of unbalance (g) and Bearing clearance (mm)	Epochs	MSE	ANN Quantification values	Percentage
1	6.5 0.08	5	3.84119e-006	6.4997 0.0799	99.99 99.87
2	10.5 0.08	9	0.000434118	10.4989 0.0797	99.98 99.62
3	14.5 0.08	3	0.00041011	14.4999 0.0798	99.99 99.75
4	18.5 0.08	6	2.89854e-005	18.4998 0.0799	99.99 99.87

Table 4 shows the normalized values of wavelets of combined faults of unbalance and bearing clearance. The first three rows of data [(6.5g+0.08mm) to (14.5g+0.08mm)] have been used for training the network and the last row of data (18.5g to 0.08mm) is test data. The network has used 6 neurons with error goal of 0.0001. The testing set has been shown in the last row of Table 4. After sum squared error has decreased and  $\mu$  has increased it yielded good generalization. 99.99 % and 99.87 % of the experimental value. The result as shown in Table 5.

### VI. Conclusions

The amplitude of vibration of a rotor bearing system, which is measured in the horizontal, vertical and axial directions, is used to study the effects of vibration characteristics of a combination of unbalance and bearing clearance. The experiments are carried out by creating crack depth ranging from 1.5mm to 6.0mm by varying the unbalance mass. It is recorded that the 1X frequency component of vibration has predominantly increased in the horizontal direction in all the cases. To quantify these faults one promising approach is to use the artificial neural network of multilayer feed forward back propagation algorithm. It has been seen by training of network with data that was obtained experimentally and by testing the same data. Further work needs to be done by using other types of networks and algorithm. Removing arbitrariness in the choice of the network parameters is another area where more work must be done. The ANN is used for diagnosing and quantifying of faults. The success rates, based upon each fault, have been reported. In particular, overall success rates of unbalance of 99.78 % unbalance, 99.81% bearing clearance, and 99.45 % for the combined faults of unbalance and bearing clearance have been achieved. This paper has also investigated the feasibility of applying discrete wavelet transform to identify the combined faults of unbalance mass and bearing clearance. To alleviate the frequency-invariant characteristics of the wavelet coefficients and to reduce the dimensionality of the input to the neural network, the RMS value at selected decomposition levels are used as a feature measure of the signal. The features obtained by the proposed method yields nearly 99.99% quantification when used as input to a Neural Network.

### REFERENCES

- [1] Dutt, J. K. and Nakra, B. C., Stability of Rotor System with Viscoelastic Support, Journal of Sound and Vibration, 153 (1), (1993), 89–96.
- [2] Genta, G. and De Bona, F. Unbalance Response of Rotors; A Modal Approach with Some Extensions to Damped natural Systems, Journal of Sound and Vibration, 140 (1), (1990), 129–153.
- [3] S. Edwards, A. W. Lees, and M. I. Friswell. Fault Diagnosis of Rotating Machinery, The Shock and Vibration Digest, 30 (1), (1998), 4-13.
- [4] Gasch, R., A survey of the dynamic Behavior of a Simple Rotating Shaft with a Transverse Crack, Journal of Sound and Vibration, 160 (2), (1993), 313-332.
- [5] Meng, G. and Hahn, E. J., Dynamic Response of Cracked Rotor With some Comments on Crack Detection, Journal of Eng. Gas Turbines and Power, 119 (2), (1997), 447–455.
- [6] Isermann, R., Supervision, Fault detection and Fault-Diagnosis methods, Control Eng. Practice, 5(5), (1997), 639–652,
- [7] A.W. Lees and M. I. Friswell, The Evaluation of Rotor Imbalance in Flexibly Mounted Machines, Journal of Sound and Vibration, 208(5), (1997), 671-683.

- [8] D. L. Hall, R. J. Hansen and D. C. Lang , The Negative Information Problem in Mechanical Diagnostics , Journal of Eng. for Gas Turbines and Power, 119,(1997) , 370-377.
- [9] K. S. Srinivasa, Fault Diagnosis in Rotating Machines Using Vibration Monitoring and Artificial Neural Networks, Ph. D Thesis, ITMMEC, Indian Institute of Technology Delhi, (2003).
- [10] K. S. Srinivasan and Umesh K. N., Study of effects of Misalignment on vibration Signatures of Rotating Machinery, National Conf. README-05, PACE, Mangalore,(2005).
- [11] A. C. McCormick and A. K. Nandi, A Comparison of Artificial Neural networks and other statistical methods for rotating machine condition classification, IEE, savoy London, (1996), 2(1)-2(6).
- [12] A. C. McCormick and A. K. Nandi, Classification of the rotating machine condition using artificial neural networks, Proceedings Instrumentation Mechanical Engineers, 211, Part-C, (1997) , 439-450.
- [13] Nalinaksh S.Vyas and D. Sathish kumar, Artificial Neural Network Design for Fault identification in Rotor-Bearing System, 36, Mechanism and Machine Theory, (2001), 157-175.
- [14] M. Kalkat and S.Yildirim and I. Uzmay , Rotor Dynamics Analysis of Rotating Machine Systems using Artificial Neural Networks, International Journal of Rotating Machinery, 9, (2003), 255-262.
- [15] Nahvi and M. Esfahanian, Fault identification in rotating machine condition using artificial neural networks, Proceedings Instrumentation Mechanical Engineering Science, 219, (2004), 141-158.
- [16] .Jeong Soo Ryu, Doo Byang Yoon and Jong sup wu, Development of a HANARO Vibration Monitoring System for Rotating Machinery, Proceedings of the Internal Symposium on Research Reactor and Neutron Science, (2005).
- [17] T. S. W. Chow and L. T. Jaw, city polytechnic of Hong Kong, Rotating machines Fault identification using Back-Propagation Artificial Neural Network, 405-412.
- [18] G. G. Yen and Kuo-Chung Lin, Wavelet Packet Feature Extraction for Vibration Monitoring, IEEE Transactions on Industrial Electronics, 47, no 3, (2000), 650-666.
- [19] D. Boras, M. Castila, N. Moreno and J. C. Montano, Wavelet and Neural Structure; A New Tool for Diagnostic of Power System Disturbances, IEEE, Transactions on Industry Applications, 30, no 1 (2001), 184-190.
- [20] Xie FL, Flowers G. T., Feng L. and Lawrence C., Steady State Dynamic Behavior of Flexible Rotor with Auxiliary Support from Clearance Bearing, Journal of Vibration and Acoustics, Vol. 121/79, 1999, 78-83.
- [21] D. Muller, A.G. Sheard., S. Mozumdar., and E. Lohann., Capacitive measurement of compressor and turbine blade tip to casing running clearance, Journal of engineering for gas turbines and power , Vol. 119, Oct 1997, 877-884.
- [22] Sang-Kyu Choi, and Sherif T. Noah., Mode locking and chaos in a Jeffcott rotor with bearing clearances, Journal of applied mechanics, vol. 61, Mar. 1994, 131-138.